

University of Nebraska - Lincoln
DigitalCommons@University of Nebraska - Lincoln

Biological Systems Engineering: Papers and
Publications

Biological Systems Engineering

6-2018

Tradeoffs in Model Performance and Effort for Long-Term Phosphorus Leaching Based on In Situ Field Data

Ryan P. Freiberger
University of Nebraska-Lincoln, rfreibe1@gmail.com


Derek M. Heeren
University of Nebraska-Lincoln, derek.heeren@unl.edu

Dean E. Eisenhauer
University of Nebraska-Lincoln, deisenhauer1@unl.edu

Aaron R. Mittelstet
University of Nebraska-Lincoln, amittelstet2@unl.edu

Guillermo Baigorria
University of Nebraska-Lincoln, gbaigorria@unl.edu

Follow this and additional works at: <https://digitalcommons.unl.edu/biosysengfacpub>

 Part of the [Bioresource and Agricultural Engineering Commons](#), and the [Environmental Engineering Commons](#)

Freiberger, Ryan P.; Heeren, Derek M.; Eisenhauer, Dean E.; Mittelstet, Aaron R.; and Baigorria, Guillermo, "Tradeoffs in Model Performance and Effort for Long-Term Phosphorus Leaching Based on In Situ Field Data" (2018). *Biological Systems Engineering: Papers and Publications*. 554.
<https://digitalcommons.unl.edu/biosysengfacpub/554>

This Article is brought to you for free and open access by the Biological Systems Engineering at DigitalCommons@University of Nebraska - Lincoln. It has been accepted for inclusion in Biological Systems Engineering: Papers and Publications by an authorized administrator of DigitalCommons@University of Nebraska - Lincoln.

Original Research

Core Ideas

- Numerical models were calibrated with in situ infiltration and leaching data.
- We evaluated how increasing model complexity improves predictions.
- Critical parameters included field-measured hydraulic conductivity and dispersivity.
- A one-dimensional dual-porosity model was adequate for long-term simulations.

R.P. Freiberger, D.M. Heeren, D.E. Eisenhauer, and A.R. Mittelstet, Dep. of Biological Systems Engineering, Univ. of Nebraska–Lincoln, 223 L. W. Chase Hall, Lincoln, NE 68583; G.A. Baigorria, School of Natural Resources, Univ. of Nebraska–Lincoln, 823 Hardin Hall, Lincoln, NE, 68583. *Corresponding author (derek.heeren@unl.edu).

Received 26 Dec. 2017.

Accepted 29 Mar. 2018.

Citation: Freiberger, R.P., D.M. Heeren, D.E. Eisenhauer, A.R. Mittelstet, and G.A. Baigorria. 2018. Tradeoffs in model performance and effort for long-term phosphorus leaching based on in situ field data. *Vadose Zone J.* 17:170216. doi:10.2136/vzj2017.12.0216

© Soil Science Society of America. This is an open access article distributed under the CC BY-NC-ND license (<http://creativecommons.org/licenses/by-nc-nd/4.0/>).

Tradeoffs in Model Performance and Effort for Long-Term Phosphorus Leaching Based on In Situ Field Data

R.P. Freiberger, D.M. Heeren,* D.E. Eisenhauer, A.R. Mittelstet, and G.A. Baigorria

Phosphorus and N are critical nutrients for agriculture but are also responsible for surface water enrichment that leads to toxic algal growth. Although P loading to surface waters has traditionally been thought to occur primarily in surface runoff, contributions from subsurface transport can also be significant. The primary objectives of this research were to evaluate several methods of representing macropore flow and transport in a finite element model using plot-scale infiltration and leaching data and to compare several models of various levels of complexity to simulate long-term P leaching. To determine flow and transport parameters, single- and dual-porosity models in HYDRUS-2D were calibrated with infiltration, Cl^- , and P data from a 22-h plot-scale leaching experiment on a silt loam mantle with gravel subsoil. Both homogeneous and heterogeneous gravel profiles were simulated. The dual-porosity model with heterogeneous hydraulic conductivity best matched experimental data, with physical nonequilibrium (dual porosity) being more important than two-dimensional (2D) heterogeneity. Long-term (9 yr) P leaching to the water table (3 m below the soil surface) at the field site was simulated with both one-dimensional (1D) and 2D models using the calibrated parameters. There was little difference between analogous 1D and 2D models, suggesting that HYDRUS-1D may be sufficient to model long-term P leaching. Overall, the most important elements for accurately simulating P leaching in this silt loam and gravel soil profile were found to be (i) field-measured hydraulic conductivity of the limiting soil layer, (ii) calibrated dispersivity, and (iii) dual-porosity, in some circumstances.

Abbreviations: BTC, breakthrough curve; EPC, equilibrium phosphorus concentration; NSE, Nash–Sutcliffe efficiency; 1D, one-dimensional; 2D, two-dimensional.

Phosphorus and N are important nutrients for crop growth and development, but overloading of freshwater systems with nutrients can induce significant algae growth. Algal blooms and cyanobacteria outbreaks contribute to hypoxic waters and fish kills, as well as reduce the quality of water for consumption and recreational use (Lopez et al., 2008). The importance of surface water quality is highlighted by litigation, including attempts to regulate nonpoint-source pollution under the Comprehensive Environmental Response, Compensation, and Liability Act, as well as the Resource Conservation and Recovery Act (Freiberger, 2014).

Phosphorus is often the limiting nutrient in surface waters (Correll, 1999). Phosphorus transport has been assumed to take place primarily in surface runoff, although a growing collection of research indicates that subsurface P transport can be significant (Osborne and Kovacic, 1993; Cooper et al., 1995; Gburek et al., 2005; Fuchs et al., 2009). At field sites in the St. Joseph River watershed in northeastern Indiana, Smith et al. (2015) found that approximately half of the P losses occurred through tile drainage, due in part to macropore flow. There is a need to be able to perform long-term simulations of P leaching to estimate long-term loading of P to aquifers and streams through subsurface transport processes.

It has been shown that, in porous media with heterogeneous flow properties, the majority of the flow can occur in small preferential flow paths (Gotovac et al., 2009; Najm et al., 2010), with potential for rapid leaching of solutes through soil profiles to groundwater. Djodjic et al. (2004) performed experiments on P leaching through undisturbed soil columns

and stressed the need to consider larger scale leaching processes due to soil heterogeneity. Subsurface P transport rates in Ozark floodplains have been shown to be comparable with surface runoff P transport rates (Mittelstet et al., 2011). In many gravelly floodplains, gravel outcrops and macropores are present, resulting in high infiltration rates, some of which are reported to be 10 to 74 cm h⁻¹ (Heeren et al., 2015). Using plot-scale solute injection experiments, Heeren et al. (2017) found P leaching from the soil surface to the groundwater to be significant, with rapid detection of P in gravel outcrops (e.g., 4 min) and in silt loam soils with macropores. In one silt loam plot, the maximum transport velocity for soluble reactive P was 810 cm h⁻¹. However, these field experiments were relatively short (3–52 h) and did not document long-term P leaching.

One way to conceptualize macroporosity in a soil is through the use of a multidomain system (Beven and Germann, 1982; Šimůnek and van Genuchten, 2008). Multidomain models split the soil profile into a fracture (macropore) domain and a matrix domain to simulate rapid flow and transport rates due to macroporosity. Multidomain models express physical transport in several ways. Mobile–immobile models define water and solute flow through the macropore space, with solute transport also occurring between the immobile and mobile domains through molecular diffusion. Dual-porosity models build on this further by allowing both water flow and solute transport (through advection as well as diffusion) to occur between the mobile and immobile domains.

HYDRUS-1D and HYDRUS-2D simulate the transport of water, solutes, and heat through simple and complex soil profiles. HYDRUS uses numerical methods (finite element in space and finite difference in time) to solve the Richards equation for variably saturated water flow and the advection–dispersion equation for heat and solute transport (Šimůnek and van Genuchten, 2008; Šimůnek et al., 2012). HYDRUS has been used to simulate preferential flow and transport both by using multidomain models that express domains as overlapping continua (e.g., dual-porosity) and by simulating a macropore as a single band of highly conductive material built directly into the finite element mesh (Akay et al., 2008; Lamy et al., 2009).

Elmi et al. (2012) used HYDRUS-1D and a single-porosity model to simulate P transport through undisturbed soil cores. Naseri et al. (2011) also performed column experiments on soils cores to measure P transport. However, neither of these studies simulated preferential flow in HYDRUS. Limited research has been performed using profile data from advanced tools, such as electrical resistivity mapping, to determine a two-dimensional (2D) saturated hydraulic conductivity (K_s) field for simulating P transport in HYDRUS. There is a need to develop long-term nutrient leaching models based on field experiments that capture the complexities of macropore flow in situ.

The objectives of this research were (i) to evaluate several methods of representing macropore flow and transport in a 2D finite element model using plot-scale infiltration and leaching data, and (ii) to compare multiple numerical models of various complexities to simulate long-term P leaching. It was hypothesized that using a dual-porosity model and accounting for spatial heterogeneity in

K_s , as well as using field measured data, would improve the ability of the model to perform accurate long-term simulations. Although increasing model complexity may improve the predictive capabilities of the model, the level of improvement needs to be compared with the effort required to calibrate more complex models.

Materials and Methods

Field Site

The Barren Fork Creek floodplain site (35.90° N, 94.85° W) was located in the Ozark ecoregion of northeastern Oklahoma. The Barren Fork Creek is a state-designated Scenic River and is on the Oklahoma 303(d) list for nutrient impairment (USEPA, 2015). Poultry feed, and thus poultry litter, is the largest source of P in the watershed (Mittelstet and Storm, 2016). Floodplains generally consist of coarse chert gravel overlaid by a mantle of gravelly loam or silt loam (Fig. 1). The soils were Razort gravelly loam (fine-loamy, mixed, active, mesic Mollic Hapludalfs) with the silt loam layer ranging from 30 to 200 cm thick and the chert gravel layer ranging from 3 to 5 m thick, extending down to limestone bedrock. The gravel vadose zone had K_s values ranging from 550 to 1700 cm h⁻¹ according to in situ borehole permeameter tests (Miller et al., 2014). The gravel itself was a complex alluvial deposit that included both clean gravel lenses associated with rapid flow and transport (Fox et al., 2011) and layers of fine gravel that could cause lateral flow in the silt loam and subsequent seepage erosion (Fig. 1). The anisotropic horizontal layering resulted in a propensity for lateral flow.

Numerical simulations used data from a previous plot-scale infiltration experiment implemented at the Barren Fork Creek site. The berm infiltration method (Heeren et al., 2014) was used to confine water and solutes in an infiltration plot (1 by 1 m) within the floodplain (Fig. 2). A constant head of water and constant Cl⁻ and P concentrations were maintained within the plot. The Cl⁻ (conservative) was injected as KCl, resulting in a concentration of 50.1 mg L⁻¹ Cl⁻. The P (highly sorbing) concentration of 1.68 mg L⁻¹ (corresponding to 5.6 mg L⁻¹ as phosphate) was used to represent poultry litter application rates (typically used as a fertilizer source in the Ozark ecoregion) in the range of 2 to 8 Mg ha⁻¹. The P concentrations were achieved by adding H₃PO₄, which deprotonated to H₂PO₄⁻ and HPO₄²⁻ in the slightly acidic solution. Five observation wells were installed near the plot to collect water samples to document solute breakthrough curves (BTCs). The infiltration data were presented in Heeren et al. (2015) and the transport data in Heeren et al. (2017). The current research used HYDRUS to simulate the 1- by 1-m infiltration plot that was tested on 30 June 2011 (Fig. 2).

Soil Chemistry

To determine soil chemical properties, soil core samples were collected with a Geoprobe Systems 6200 TMP (trailer-mounted probe) direct-push drilling machine using a dual-tube core sampler with a 4.45-cm opening. Before the P injection experiment, background soil cores were collected during the installation of the observation wells and were tested for water-soluble P. After the P injection experiment, soil cores were collected from within the plot



Fig. 1. Streambank at the Barren Fork Creek field site including the bank profile (top left), a megapore (top right), and a seepage undercut (bottom). Note the sloughed material at the bottom of each picture from recent bank failures. These complex alluvial deposits include both clean gravel lenses associated with rapid flow and transport (top left) and fine gravel lenses that can cause lateral flow and seepage erosion (bottom).

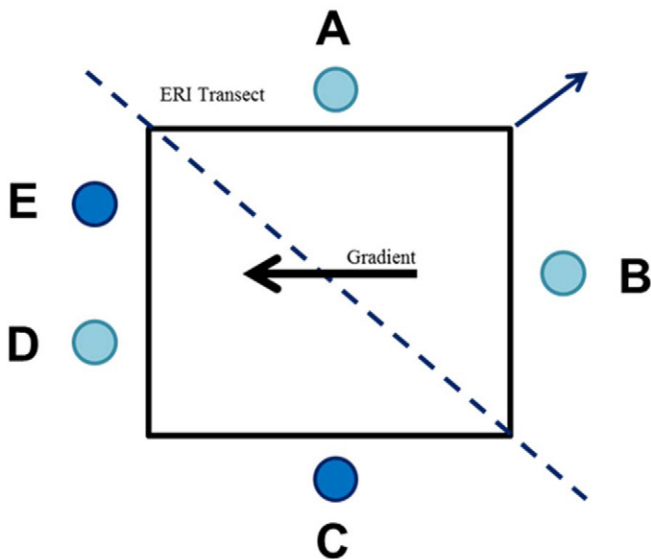


Fig. 2. Overhead view of the infiltration plot (square) used for model calibration. Observation wells (circles) are labeled A through E, with the dark blue wells selected for calibration. The blue arrow indicates north, and the black arrow shows the direction of groundwater flow. The dashed line is the location of the vertical electrical resistivity imaging (ERI) profile used to quantify spatial variability in hydraulic conductivity.

to document the change in the soil profile water-soluble P levels due to the infiltration of P-laden water (Fig. 3). All soils were air dried and sieved with an 8-mm sieve prior to analysis. Details of the laboratory testing are presented in Heeren et al. (2017).

Isotherms were performed on samples (<8-mm fraction) from the soil cores near the infiltration plot (Table 1). The P isotherms exhibited linearity at low concentrations (<8 mg L⁻¹) and were fit with a linear isotherm (Heeren et al., 2017). The equilibrium P concentration (EPC), where neither sorption nor desorption occurred, was calculated as the *x* intercept of a logarithmic trend line fit to the entire data set (including high concentrations) (Table 1). Although the EPC was high (0.94–1.08 mg L⁻¹) compared with the background P concentrations in the aquifer (0.055 mg L⁻¹), the EPC was lower than the P concentration of the infiltrating water during the field experiment (1.68 mg L⁻¹).

The isotherms were performed on the fine fraction (<8 mm); however, parameters were needed that characterized the whole soil sample, since HYDRUS calculates P sorption in terms of the entire soil mass. Sorption on the coarse size fraction (>8 mm) was assumed to be negligible (Heeren et al., 2017). Therefore, “weighted” linear isotherm parameters were determined by accounting for the fraction of total sample on which testing was performed:

$$K_{d,whole} = f_{<8mm} K_{d,<8mm} \quad [1]$$

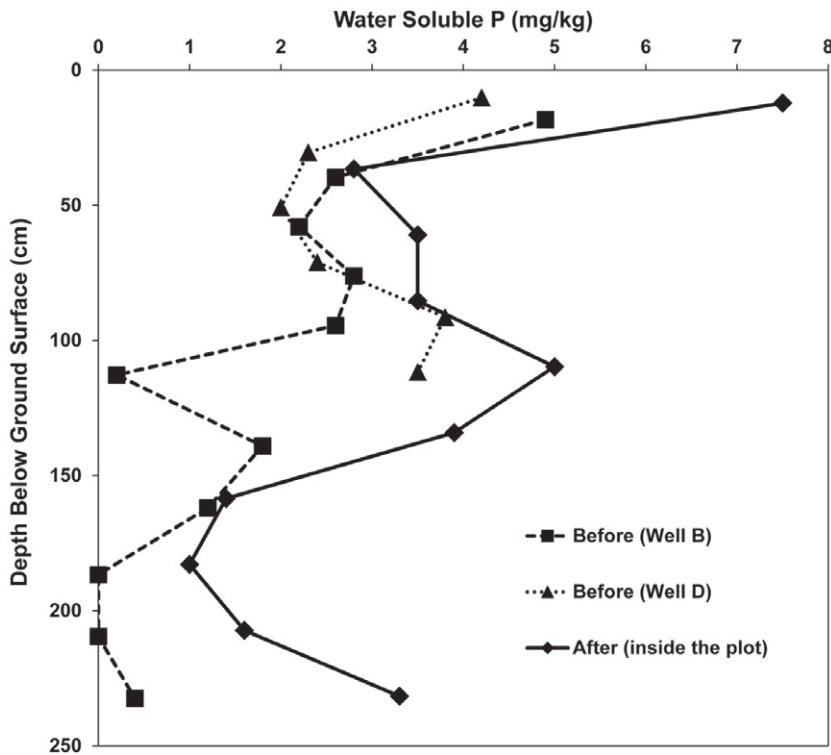


Fig. 3. Subsurface soil water soluble P concentrations (mg P kg^{-1} soil) before and after the infiltration experiment. Note the location of the concentration front between 160 and 185 cm (Well B).

where $K_{d, \text{whole}}$ is the linear sorption coefficient for the whole soil sample (L water kg^{-1} soil), $f_{<8\text{mm}}$ is the fraction of the soil sample that passes through an 8-mm sieve (kg kg^{-1}), and $K_{d, <8\text{mm}}$ is linear sorption coefficient for the fine fraction (L water kg^{-1} soil) (Table 1). The $y_{\text{int, whole}}$ (where the line of the weighted isotherm intercepted the y axis, mg P kg^{-1} soil) was also weighted according to $f_{<8\text{mm}}$. The EPC was the same for the fine fraction and the entire sample.

Numerical Simulations

Numerical methods were used to solve the Richards equation and the advection–dispersion equation for variably saturated flow and transport within HYRUS-1D and -2D, using both single- and dual-porosity formulations (Table 2). Model A was designed to use the level of data that would be available from a quick field site visit, including visual observation of silt loam and gravel layering on the streambank, a bucket sample of gravel (from the streambank) to determine the particle size distribution, and soil coring in the floodplain to determine depth of the silt loam, soil texture, water-soluble P, and P sorption isotherms. If successful, this single-porosity, one-dimensional (1D) model would require

relatively little effort to implement at other field sites. Model B used measured K_s (from an infiltration experiment for the silt loam and from a borehole permeameter for the gravel) and calibrated longitudinal dispersivity (D_L). Model B was 2D, although both the silt loam and the gravel were homogenous. Model C was designed to use data collected from an in-depth study of the research site. Model C accounted for heterogeneity in the gravel with three gravel layers, according to electrical resistivity imaging of the vadose zone. Due to the highly complex alluvial deposits (Fig. 1), it was expected that accounting for 2D heterogeneity in soil properties would significantly improve model performance.

Models D and E used a dual-porosity model to simulate the impact of preferential flow. Both models used measured K_s , calibrated D_L , and calibrated dual-porosity parameters. Model E required the most field data and modeling effort, using both dual-porosity and 2D heterogeneity in K_s .

Soil Physical Properties

The vertical soil profile was divided into two distinct soil layers—a 1.33-m silt loam layer and an underlying layer of

Table 1. Soil chemical properties for two soil samples from soil cores near the field infiltration experiment. The linear sorption coefficient (K_d) and y intercept are the best-fit line for the linear P isotherms. The weighted K_d was used to simulate P sorption in the silt loam and gravel in the numerical models. Adapted from Heeren et al. (2017).

Borehole	Depth	Soil texture	8-mm sieve	EPC†	<8-mm fraction		Weighted	
					K_d	y intercept	K_d	y intercept
	cm		% passing	mg L^{-1}	L kg^{-1}	mg kg^{-1}	L kg^{-1}	mg kg^{-1}
Well B	64–83	Silt loam, some gravel	94	0.94	11	–14	10	–13
Well K	142–163	Sandy gravel	57	1.08	2.6	–6.3	1.5	–3.6

† EPC, equilibrium P concentration.

Table 2. Description of models used to simulate flow and transport.

Model	Porosity†	Dimension‡	K_s §		D_L ††	Application‡‡
			Silt loam¶	Gravel#		
A	SP	1D	PTF	PSD-HM	Lit	LT
B	SP	2D	Meas	Meas-HM	Cal	Cal
C	SP	2D	Meas	Meas-HT	Cal	LT, Cal
D	DP	1D	Meas	Meas-HT	Cal	LT
E	DP	2D	Meas	Meas-HT	Cal	LT, Cal

† SP, single porosity; DP, dual porosity.

‡ 1D, one-dimensional; 2D, two-dimensional.

§ K_s , saturated hydraulic conductivity.

¶ PTF, K_s estimated with pedotransfer function (Rosetta Lite); Meas, measured with plot infiltration experiment.

PSD, K_s estimated by particle size distribution; HM, homogeneous with a single gravel layer; Meas, measured with borehole permeameter and electrical resistivity imaging; HT, heterogeneous with three gravel layers.

†† D_L , longitudinal dispersivity; Lit, D_L according to literature; Cal, calibrated D_L .

‡‡ LT, long-term simulations; Cal, calibration simulations.

gravel—based on the layering at the field site. Values for van Genuchten parameters and soil material properties for the soil layers were estimated using the Rosetta Lite (version 1.1) module. Gravel soil parameters were estimated using the “sand” classification in Rosetta Lite, since parameters were not available for gravel. The silt loam K_s value was estimated to be 9.6 cm h^{-1} from the field infiltration tests (Heeren et al., 2015).

Flow and transport are highly complex, 2D or three-dimensional processes (Fig. 1) (Heeren et al., 2017). This research sought to improve model performance by accounting for spatial heterogeneity in soil properties by using a 2D simulation informed by geophysics. The gravel was divided into three layers identified using electrical resistivity imaging data (Miller et al., 2014, 2016) from the location of the plot. The K_s (m d^{-1}) values for the gravel layers were determined using electrical resistivity data and the relationship below, which was developed using borehole permeameter data from the Barren Fork Creek site and one other floodplain site in the Ozark ecoregion (Miller et al., 2014, 2016):

$$K_s = 0.11\rho \quad [2]$$

where ρ is electrical resistivity ($\Omega \text{ m}$). The K_s values for points within each gravel layer, as determined with electrical resistivity data, were then averaged to generate an average K_s for that layer. Average K_s values for the three gravel layers ranged from 130 to 578 cm h^{-1} .

Soil Chemical Properties

The units in the HYDRUS simulations were centimeters for length, grams for soil mass (i.e., bulk density in g cm^{-3}), micrograms for P or Cl^- mass, and hours for time. Therefore, the linear sorption coefficient (K_d) for P was entered in units of cubic centimeters per gram (e.g., $K_d = 10.3 \text{ L kg}^{-1} = 10.3 \text{ cm}^3 \text{ g}^{-1}$ for the silt loam). The measured K_d for the gravel sample was applied to the whole gravel layer. Initial conditions included soil solution P concentrations equal to the EPC for the silt loam layer (0.94 mg L^{-1}) and the top of the gravel layer (1.08 mg L^{-1}). Initial solution P concentration in the

gravel below the water table was equal to the average of background P concentrations from well samples (0.055 mg L^{-1}). The disparity in these concentrations indicates the presence of a solute front in the soil matrix (from historical P leaching) that has not yet reached the water table, although P leaching through macropores may have reached the water table during rainfall events. Given the relative location of this solute front, which is apparent in the water-soluble P data (Fig. 3), a linear interpolation was used for the initial solution P concentration between 1.08 mg L^{-1} at 160 cm and 0.055 mg L^{-1} at 175 cm. Soil P was assumed to be in chemical equilibrium with the solution.

Calibration

During calibration, simulation results from the 2D models were matched to data collected from Observation Wells C and E adjacent to the plot (Fig. 2), which were the only two wells in which P was detected. Since the field experiments involved a 2D flow field (including lateral flow at the top of the water table before intersecting a well), it was necessary to use 2D numerical models for the calibration. Observation nodes in HYDRUS were placed at the water table on either side of the plot to represent the selected observation wells. A constant head of 6 cm was applied across the plot area. Constant concentration boundary conditions of 50.1 and 1.68 mg L^{-1} were used for Cl^- and P, respectively. Calibration was performed for the 2D models for both Cl^- and P transport. Goodness-of-fit was determined using the R^2 and Nash–Sutcliffe efficiency (NSE; Nash and Sutcliffe, 1970) as recommended by Moriasi et al. (2007). Although R^2 describes the collinearity between the observed and simulated values, it is oversensitive to outliers and insensitive to additive and proportional differences between model predictions and measured data (Legates and McCabe, 1999). Nash–Sutcliffe efficiency, with a range from $-\infty$ to 1.0, indicates how well the plot of observed vs. simulated data fits the 1:1 line.

The numerical simulations included several levels of input data (Table 2). Models B and C were performed using the default single-porosity van Genuchten–Mualem 2D model, both with a homogeneous gravel (Model B) and heterogeneous gravel (three

gravel layers, Model C). Additional models were included to evaluate the effects of incorporating macropore flow (dual-porosity) on arrival time and the overall shape of Cl^- and P BTCs.

Single-Porosity Parameters

Dispersivity [L] is used to correlate pore velocity to the mechanical dispersion of solutes in porous media. Traditionally, D_L has been approximated to be 10% of the sample length in the direction of flow, with transverse dispersivity (D_T) being $\sim 10\%$ of the D_L (Lallemand-Barres and Peaudecerf, 1978; as presented in Fetter, 1999). The flow path length during the field experiments was ~ 400 cm, resulting in a first estimate of D_L of 40 cm for the calibration. The D_T was always calculated to be 10% of the D_L .

Dual-Porosity Parameters

For the dual-porosity models, the $\theta_{s,mo}$ and $\theta_{s,im}$ [$\text{L}^3 \text{L}^{-3}$] are the saturated volumetric water contents of the mobile and immobile domains. Tension infiltrometer tests conducted by Heeren et al. (2015) showed that 99% of flow was directed through macropores at the Barren Fork Creek site. Simulations conducted by Šimůnek et al. (2003) suggested the possibility of such flows occurring through a mere 2.5% of total pore space, which suggested that macropores can have a dominant effect on subsurface flows. Furthermore, Haws et al. (2005) modeled 2D mobile zones as a small percentage of the total porosity. Reducing the flow domain to such a small space has dramatic effects on mean pore water velocity, causing water and solutes to arrive much sooner than arrival after flowing through simple matrix flow. Values of $\theta_{s,mo}$ and $\theta_{s,im}$ were initially set to reflect the simulation conducted by Šimůnek et al. (2003), and $\theta_{s,mo}$ was allowed to be adjusted between 0.01 and the porosity estimated by the Rosetta Lite function (Table 3).

The ω [T^{-1}] and α [T^{-1}] terms are the water and solute mass transfer coefficients, respectively, for the mass transfer function in the modified advection–dispersion equation. Values of α are traditionally believed to range between 0.1 and 5.0 h^{-1} (Radcliffe and Šimůnek, 2010); however, Alletto et al. (2006) found α to range between 0.0006 and 0.0424 h^{-1} , and Cheviron and Coquet (2008) reported α values of 0.0192 to 0.6528 h^{-1} . González-Delgado and Shukla (2014) reported ω values of 0.001 to 0.30 h^{-1} in loam and 0.20 to 1.02 h^{-1} in sand. Therefore, BTCs were analyzed with ω ranging by several orders of magnitude with a minimum of 0.001 for both silt loam and gravel (Table 3).

The $f[-]$ is the fraction of sites available for sorption that are governed by an equilibrium process. Given the mobile–immobile nature of this particular model, f was used to denote the fraction of sites in contact with mobile water during physical nonequilibrium. We analyzed f for the entire range of possible values to get a good understanding of its effect on P sorption (Table 3). Due to the conservative nature of Cl^- , f was not calibrated when simulating Cl^- transport.

Sensitivity Analysis

A sensitivity analysis was conducted on Model E to determine the impact of each parameter on arrival time for both Cl^- and P

transport. The best-fit parameter values (Table 3) were used to set the baseline parameter values for the sensitivity analysis. Each solute simulation was analyzed with respect to the time taken for water at the Well C observation node to reach a concentration of 15 mg L^{-1} for Cl^- (t_{15}) or 0.12 mg L^{-1} for P ($t_{0.12}$). Input parameters were then increased or decreased, and the percentage change in t_{15} or $t_{0.12}$ was recorded. Results were plotted as the percentage change in the parameter from the baseline value vs. the percentage change in time to the target concentration.

Long-Term Phosphorus Simulations

Long-term P transport was simulated with both the 1D and 2D calibrated models. Long-term trials simulated water and P application to a soil profile for a 9-yr period between March 2004 and March 2013. Rainfall data were obtained through the Oklahoma Mesonet (McPherson et al., 2007). Since the focus of this research was a comparison of model performance, rather than the magnitude of P load to the aquifer, evapotranspiration was neglected in the simulations. Future research should account for root water and nutrient uptake (Šimůnek et al., 2016) when simulating P leaching.

Phosphorus from poultry litter application was simulated as P applied with infiltrating rainwater starting 1 March of each year to match traditional fertilizer application times. Each year, $0.619 \text{ mg P cm}^{-2}$ of soil surface was added to the simulation, consistent with a 5 Mg ha^{-1} (2 t acre^{-1}) application rate of poultry litter on grass and a P content of 12.7 kg P t^{-1} of litter, as recommended by the Oklahoma Cooperative Extension Service (OCES,

Table 3. Soil properties and calibration parameters. The most optimal parameter set was achieved using Model E.

Soil	K_s	van Genuchten parameter†				
		Mobile			Immobile	
		α	n	l	α	n
	cm h^{-1}	cm^{-1}			cm^{-1}	
Silt loam	9.6	0.1	2.00	0.5	0.020	1.41
Gravel	130–578	0.145	2.68	0.5	0.145	2.68
Calibration parameter range‡						
	$\theta_{s,mo}$	D_L	D_T	ω	α	f
	$\text{cm}^3 \text{cm}^{-3}$	cm	cm	h^{-1}		
Silt loam	0.01–0.45	4–200	0.4–20	0.001–1	0.001–5	0–1
Gravel	0.01–0.43	4–200	0.4–20	0.001–10	0.001–5	0–1
Most optimal parameter set						
	$\theta_{s,mo}$	D_L	D_T	ω	α	f
	$\text{cm}^3 \text{cm}^{-3}$	cm	cm	h^{-1}		
Silt loam	0.01	100	10	0.01	0.2	1
Gravel	0.01	200	20	0.1	0.01	1

† α , parameter for the retention curve; n , parameter for the retention curve; l , pore connectivity parameter for unsaturated hydraulic conductivity.

‡ $\theta_{s,mo}$, saturated volumetric water content of the mobile domain; D_L , longitudinal dispersivity; D_T , transverse dispersivity; ω , water mass transfer coefficient; α , solute transfer coefficient; f , fraction of sites available for sorption.

2013). Initial concentrations of P in the simulated infiltration started at 15 mg L^{-1} , which is consistent with P concentrations in the first post-litter-application runoff event found by DeLaune et al. (2004). The decay of runoff P concentrations was simplified as a linear relationship between concentration and cumulative rainfall:

$$C = I - 0.182R \quad [3]$$

where C is the concentration (mg L^{-1}) at the given time step, I is 15 mg L^{-1} , the initial leachate concentration at 1 March of each year (mg L^{-1}), and R is the cumulative rainfall (cm) since 1 March of each year. Once the cumulative applied P reached 0.619 mg , no additional P was added to rainwater for that year. If rainfall was insufficient to remove all P from the surface for a given year, the excess P was added to the next year and a new linear relationship was developed to reflect the additional P.

Two long-term simulations were performed in HYDRUS-1D. Model A was designed to use the level of data that would be available from a quick site visit, and Model D included dual porosity to account for preferential flow. For Model A, the soil profile featured a 1.33-m silt loam mantle and a single 1.66-m gravel layer. Most of the soil characteristics for the gravel layer were defined as sand by Rosetta Lite, although the K_s value was determined using data collected by Fuchs et al. (2009) for the Barren Fork Creek site. The D_L was set to 10% of the length of the flow path (3 m); therefore, D_L was 30 cm for Model A. For Model D, the gravel layer was broken into three distinct layers. Model D evaluated transport with calibrated values for the rate constants and D_L .

For 2D modeling, a 100-cm-wide, 300-cm-deep 2D domain was developed, corresponding to the vadose zone of the soil profile directly under the 100-cm-wide plot used in calibration. Long-term P transport to the water table, situated at the bottom of the profile, was of interest. Boundary conditions were set so that the sides of the domain were no-flow boundaries, the bottom of the domain was a constant head boundary (pressure head equal to zero) at the water table elevation, and the top of the domain was set as a variable flux boundary to simulate rainfall events. Initial conditions were at hydrostatic equilibrium with the water table, and initial concentrations remained the same as the initial concentrations used for P calibration. Long-term 2D simulations were performed on Models C and E (Table 2).

Results Calibration

For Cl^- , Model E achieved the best calibration (Table 4, Fig. 4 and 5). Both R^2 and NSE were higher for Well C than Well E, 0.70 and -0.96 , respectively. The low NSE values were due to the underprediction at times 0.83 and 2.1 h. The NSE increased to 0.92 and -0.36 in Wells C and E, respectively, when only considering times 8.1 and 18.8 h. Overall, HYDRUS simulated P better than Cl^- . In Well C, the fit was excellent, but the concentrations were overpredicted in Well E. The single-porosity model with a homogeneous gravel layer (Model B) produced BTCs with longer arrival times,

reduced peak concentrations, and poor differentiation between the two observation wells (Fig. 4 and 5). The single-porosity model with heterogeneous gravel layers (Model C) performed slightly better. While still having poor arrival times and peak concentrations, this model showed better differentiation between the two observation wells (Fig. 4 and 5). Calibration parameters for these two models were limited to D_L and D_T for the silt loam; all other variables either belong to the dual-porosity model or were already set to their maximum value prior to calibration. Silt loam D_L and D_T were set to the maximum value established in Table 3 to produce these results. The best-fit parameter values for Model E are shown in Table 3.

Decreasing ω increased arrival time for both Cl^- and P, and increasing ω had the opposite effect. Effects of α were more complex. Decreasing α made the Cl^- BTC sharper but had little effect on arrival time; however, increasing α affected both time and shape of Cl^- BTC. No significant effect was seen in the P BTC for changes in α .

One limitation of the model was the inability to match observed data with reasonable f values. Predicted values of f were ~ 0.03 , which is consistent with the percentage macropore composition of the soil profile. However, parameter optimization resulted in f being close to one to achieve reasonable arrival times for P and remain consistent with Cl^- calibration results. Arrival times were difficult to match for Cl^- and P simultaneously. Although arrival times for Cl^- were relatively short, arrival times for P were relatively long. Balancing parameters that managed water flow, such as ω , was a difficult task, as changing these parameters to better match one solute caused a poor match with the other. Solute transport parameters, such as soil isotherm properties, were not enough to balance the Cl^- and P perfectly. Observation data showed that both wells received some level of Cl^- , but only Well C recorded any significant P increase. Although the P increase simulated in Well E was reduced in comparison with Well C, the increase simulated was still far above the trend defined by observed data (Fig. 5). These challenges may indicate the limitations of using the Richards equation to simulate the complex flow and transport processes observed in field conditions (Beven and Germann, 2013).

During the calibration, solute mass balance errors for P were $< 0.88\%$ for all time steps and models. The Cl^- mass balance errors

Table 4. Statistical calibration results for Cl^- and P transport for two-dimensional models for Wells C and E. Goodness-of-fit was evaluated using the R^2 and Nash–Sutcliffe efficiency (NSE).

Model	Statistic	Cl^-		P	
		R^2	NSE	R^2	NSE
B	Well C	0.47	-3.30	0.77	0.15
	Well E	0.47	-4.93	0.83	-3.35
C	Well C	0.46	-3.44	0.77	0.15
	Well E	0.47	-5.13	0.56	-2.61
E	Well C	0.70	-0.96	0.82	0.81
	Well E	0.34	-3.32	0.85	-9.56

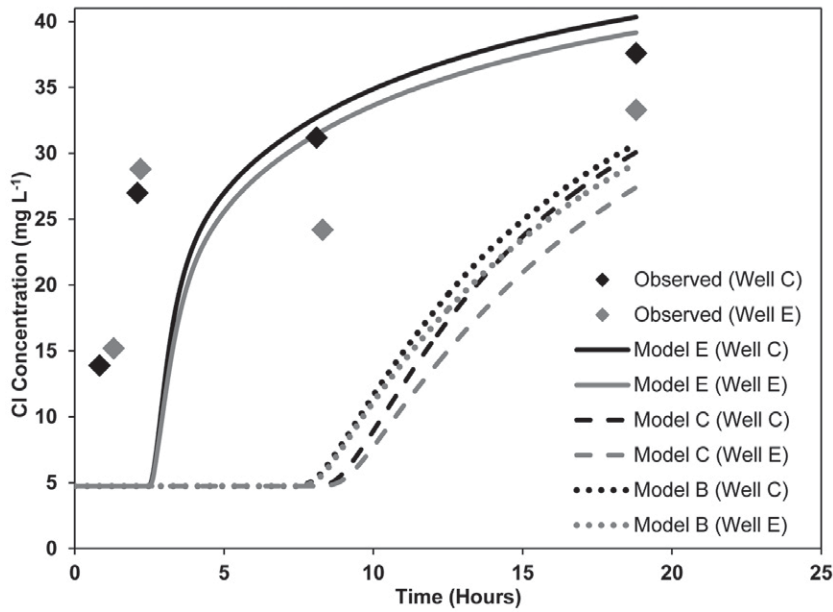


Fig. 4. Calibration of two-dimensional models with Cl^- data, including a single-porosity model with homogeneous gravel (Model B), a single-porosity model with heterogeneous gravel (Model C), and a dual-porosity model with heterogeneous gravel (Model E).

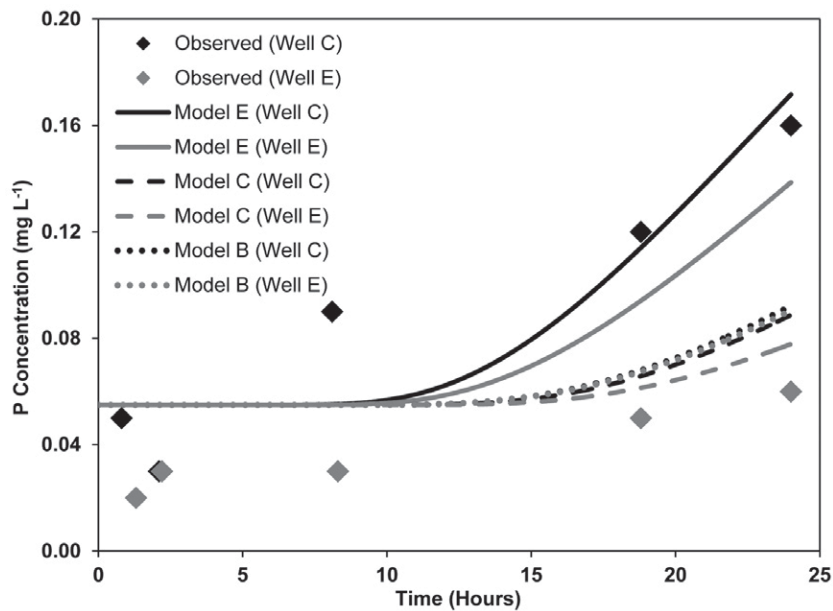


Fig. 5. Calibration of two-dimensional models with P data, including a single-porosity model with homogeneous gravel (Model B), a single-porosity model with heterogeneous gravel (Model C), and a dual-porosity model with heterogeneous gravel (Model E).

were $<3.7\%$ for all time steps and models. The water mass balance errors were $<2.1\%$ for all time steps for Models B and C, although water mass balance errors reached 24% for Model E during calibration.

Sensitivity Analysis

For Cl^- modeling, D_L and immobile pore fraction had an inverse relationship to t_{15} , whereas α and ω had a positive relationship to t_{15} , although both α and ω seemed to display asymptotic behaviors at large percentage increases in the variable. The most sensitive parameters for the Cl^- analysis were $\theta_{s,im}$ for both the silt loam and the gravel, with maximum increases in t_{15} of 77 and 167%, respectively. The least sensitive parameter was α for the silt loam, which only produced a 4% increase in t_{15} despite seeing a 400% increase in α (Fig. 6).

For P modeling, the gravel mobile sorption site fraction and the gravel adsorption isotherm coefficient had a positive relationship to $t_{0.12}$. Neither the mobile site sorption fraction nor the adsorption isotherm coefficient for the silt loam layer had any significant effect on $t_{0.12}$. Although soil chemical analysis showed that the soils were not close to P saturation (degree of P saturation $< 16\%$), initial solution P concentration in the silt loam (0.94 mg L^{-1}) was high relative to the plot inflow P concentration (1.68 mg L^{-1}). This initial condition would significantly reduce the impact of silt loam-dependent parameters, as sorption sites are already mostly filled with P for the inflow concentration. The gravel mobile sorption site fraction was the most sensitive parameter, with a maximum of 70% decrease in $t_{0.12}$. The least sensitive parameters were gravel adsorption isotherm coefficients, with changes between -20 and 20% in $t_{0.12}$ across a wide percentage change in the variable (Fig. 6).

Long-Term Phosphorus Simulations

Long-term modeling from March 2004 to March 2013 was conducted using Models A, C, D, and E. During the calibration, Model E resulted in the best fit with the field data, using a dual-porosity model and field-calibrated parameters; therefore, Model E was also considered to be the optimum model for the long-term simulations, and results from the other models were compared with Model E results.

During 9 yr, $\sim 540 \text{ kg ha}^{-1}$ P was applied to the plot area through simulated fertilizer application. Model E simulated $91.7 \text{ kg P ha}^{-1}$ being delivered to the water table, resulting in a P delivery ratio of 16.8% (Table 5). The P concentration of the flow into the water table steadily increased with time, with a final concentration of 1.74 mg L^{-1} . Wet years (2004, 2008, and 2009) resulted in larger increases in P concentration than average and dry years (Fig. 7). Model C, similar to Model E but with a single porosity, predicted a final P concentration at the water table of 1.64 mg L^{-1} .

Among the 1D models, Model D and Model E results were the most similar, with a P delivery ratio of 16.5% and a maximum P concentration of 1.67 mg L^{-1} . Model A (single porosity, without field-measured K_d) predicted that a negligible amount of P (0.2 kg P ha^{-1}) crossed the water table after 9 yr of simulation (Table 5). It is important to note that these trials do not take evapotranspiration into account; these results are intended for comparison of various models, rather than quantifying the magnitude of P leaching loads. It is expected that, if evapotranspiration was included in the model, deep percolation past

the root zone and P leaching would be proportionally less than the simulated values, with the relative differences among the various models being similar.

During the long-term simulations, the P mass balance errors were $<4.9\%$ for all time steps and models. The water mass balance errors were $<0.78\%$ for all time steps for Models A, C, and D; the maximum water mass balance error for Model E was 8.2%.

Discussion Calibration

During the calibration step, Cl^- and P transport were modeled satisfactorily (Table 4) while still keeping the values of soil properties within accepted ranges (Table 3), except for the fraction of sites available for sorption. There was some difficulty matching simulation BTCs to observed data. It is possible that the electrical resistivity imaging data could not provide a fine enough resolution of the soil profile to catch heterogeneity that would have explained why only one well displayed P transport. Another explanation might be that the dual-porosity model does not capture all of the flow and transport processes in this system and that alternative modeling techniques may be preferable (Nimmo, 2010; Beven and Germann, 2013).

The comparison of the models suggests the necessity of using a dual-porosity model to accurately represent macropore flow. During calibration, models not featuring a dual-porosity system considerably undersimulated both P and Cl^- . A single-porosity model does not adequately simulate solute transport processes, especially early arrival times, for soils dominated by macropore flow.

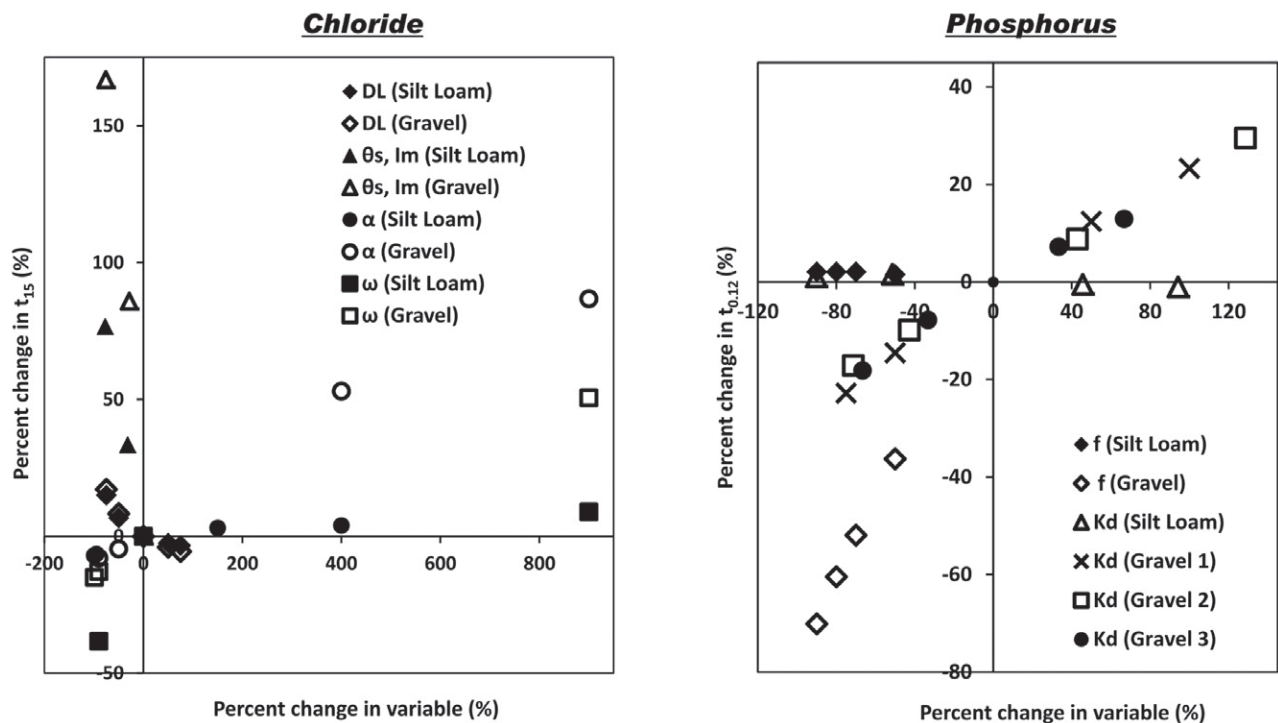


Fig. 6. Sensitivity analysis of Model E for Cl^- (left) and P (right). The model output (y axis) was selected to be comparable with the calibration dataset, with t_{15} being the breakthrough time for Cl^- to reach 15 mg L^{-1} and $t_{0.12}$ being the breakthrough time for P to reach 0.12 mg L^{-1} . DL is the longitudinal dispersivity, $\theta_{s, Im}$ is the saturated water content of the immobile domain, α and ω are the solute and water mass transfer coefficients, f is the fraction of sites available for sorption, and K_d is the linear sorption coefficient.

Table 5. Summary of long-term results for P leaching. Cumulative P delivery and final P concentrations shown are at the water table at the end of each simulation. The P delivery ratio is the ratio of the cumulative P delivered (to the water table) to the cumulative P applied (to the soil surface).

Model	Modeling effort	Cumulative P delivered [†]	P delivery ratio	Final water table P concentration [†]	Difference [‡]	
					P delivery ratio	P concentration
		kg ha ⁻¹	%	mg L ⁻¹	%	
A	Very low	0.2	0.04	0.05	-99.8	-96.8
C	High	87.1	16.0	1.64	-5.9	-5.7
D	Medium	88.5	16.5	1.67	-2.9	-4.0
E	Very high	91.7	16.8	1.74	-	-

[†] At the end of the 9-yr simulations.

[‡] Difference from Model E results.

Additional data (e.g., from a longer infiltration experiment) would have been helpful for calibrating complex models with many parameters, although long field infiltration experiments become logistically difficult. Future infiltration and leaching experiments could begin with Cl⁻ and P in the injection water but also add an additional conservative solute (e.g., Br⁻) once the water flux reaches steady state. This would allow an additional step in the model development process: calibrate flow (e.g., K_s) using infiltration data, calibrate mobile-immobile parameters (e.g., D , α , and $\theta_{s,m}$) using the data from the second conservative solute (steady flow results in no water flux between the mobile and immobile regions), calibrate the additional dual-porosity parameter (i.e., ω) using the Cl⁻ data (transient flow conditions resulting in water

flux between the mobile and immobile regions), and calibrate sorption parameters using the P data.

Long-Term Phosphorus Simulations

The 1D long-term models demonstrated the importance of several factors in long-term simulations of nutrient transport. Model A demonstrated the importance of collecting detailed soil data. Using Rosetta Lite to define soil properties, especially the silt loam K_s value, together with a single-porosity model resulted in a P load estimate over two orders of magnitude lower than the P load predicted by Model E. Conducting plot infiltration experiments or using a double-ring infiltrometer to obtain soil K_s values would be preferred over using pedotransfer functions. Model D underscored

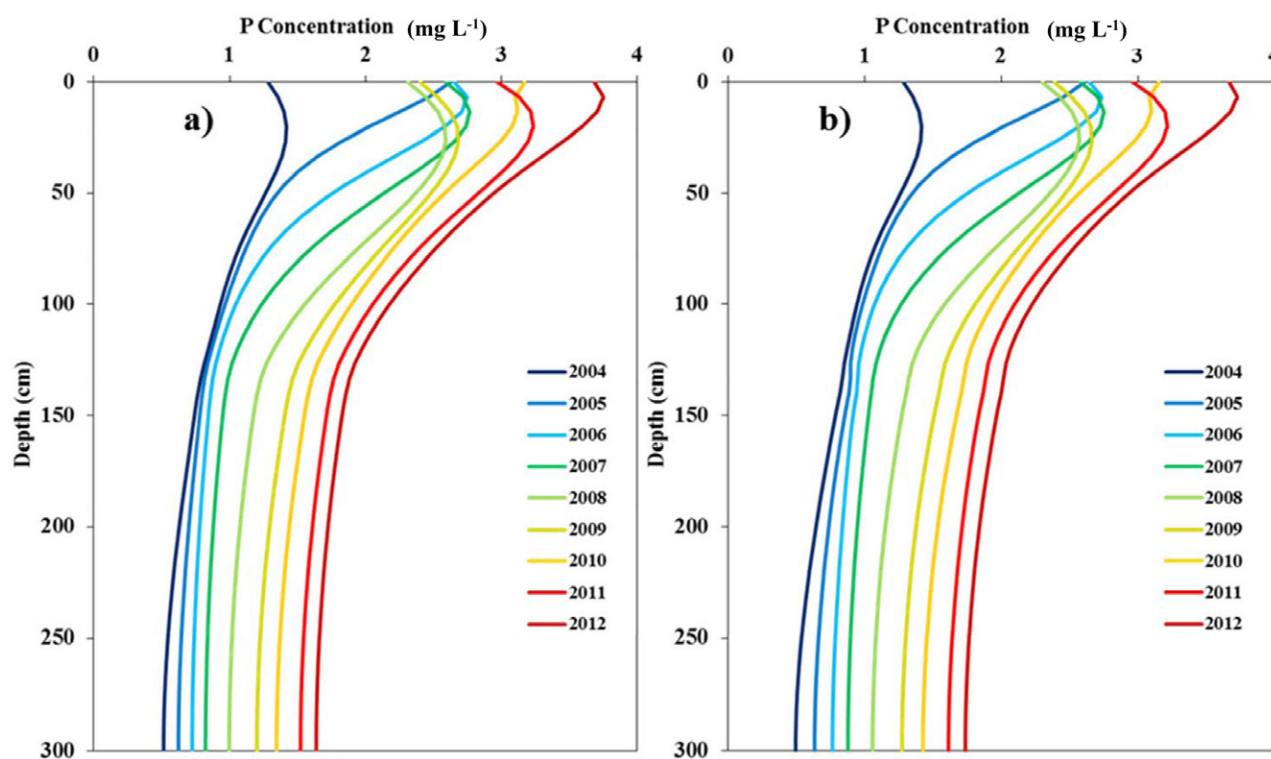


Fig. 7. Soil water P concentration profiles for (a) Model C and (b) Model E during the 9-yr simulation. Profiles were from 1 March each year. The solution P concentration was in equilibrium with the soil P concentration. Wet years included 2004, 2008, and 2009.

the value of calibrating D_L , reducing the difference in the final P concentration to -4.0% .

There was not a substantial difference between the 1D and 2D models when the 1D model was well calibrated. Specifically, Model D had a P delivery ratio only 2.9% lower than Model E, suggesting that HYDRUS-1D and -2D performed equally well in long-term simulations. This was surprising due to the high level of 2D heterogeneity at the field site (Fig. 1). However, flow was limited by the silt loam layer (treated as homogeneous in all models), and the 2D K_s data in the gravel had mostly vertical variation and little horizontal variation. The suitability of the 1D model is a significant finding because of the large amount of effort and expense required to collect geophysical data and to develop a 2D field of K_s data to inform a 2D model.

Final water table P concentrations were $\sim 2.7 \text{ mg L}^{-1}$, almost two orders of magnitude higher than the 0.037-mg L^{-1} P surface water standard set for Oklahoma Scenic Rivers. These data have implications for surface water P enrichment, especially in gravel floodplains with rapid stream–groundwater interactions.

Comparing Models C and E in the long-term 2D simulations highlighted the physical process of solute flux between the mobile and immobile zones. It was expected that the dual-porosity soil profile in Model E would deliver more P to the water table than Model C (single-porosity); however, the difference between the two models was not substantial. A possible explanation is that the solute mass transfer rate (Γ_s) is high enough to move much of the solute out of the macropore and into the matrix before solute-laden water reaches the water table, resulting in a quasi-physical equilibrium. The large value of Γ_s is influenced by two important factors in these simulations. First, the α term for the silt loam mantle is moderately high compared with ranges found in the literature. Second, the difference between the mobile and immobile concentrations ($c_{\text{mo}} - c_{\text{im}}$) is large. The matrix P concentration at the top of the soil profile is relatively low throughout the 9-yr simulation period (<1 to $\sim 3.5 \text{ mg L}^{-1}$). In comparison, the infiltrating water of the long-term simulations contained P concentrations starting at 15 mg L^{-1} at the beginning of each year and had a higher P concentration than the matrix for most of the year. In contrast, the conditions during calibration resulted in a far smaller concentration gradient, where the inflow concentration was only 1.68 mg L^{-1} . With the Γ_s term being much smaller, flux from the macropores to the matrix was limited. Therefore, the dual-porosity model simulated rapid transport of solute through the macropore to the water table, explaining the large difference between Model C and Model E during calibration (Fig. 4 and 5).

Future long-term modeling attempts should simulate additional plots and sites to create a more comprehensive analysis of each of the models studied in this research. Research could determine which model components (e.g., single vs. dual porosity) would be best suited for various combinations of soil profile, initial, and boundary conditions. Future studies simulating long-term infiltration could help watershed managers better understand the lag time for multiple other conservative and highly sorbing pollutants such

as nitrate and atrazine. Understanding this lag time is imperative to better manage water quality and legacy pollutants.

Summary and Conclusions

A numerical model was calibrated to match observed data for Cl^- (conservative) and P (highly sorbing). Of the three calibrated models, the Model E dual-porosity heterogeneous profile model matched the observed data for both solutes the best. The sensitivity analysis indicated that physical nonequilibrium input parameters ($\theta_{s,\text{im}}$ and f) were the most important, followed by dispersivity (D_L). Using a heterogeneous profile for gravel K_s (Model C) provided only a minor improvement over a homogeneous profile (Model B), despite complex soil layering.

For long-term simulations of P leaching, the most convenient model (Model A) was inadequate (two orders of magnitude low), primarily due to the pedotransfer-function-estimated K_s for the silt loam and the estimated D_L . Model C provided much better results, confirming the well-known fact that K_s needs to be measured in the field (especially for the limiting layer), and that D_L needs to be calibrated with field data. For the long-term simulations, accounting for physical nonequilibrium (the dual-porosity model) only provided a small benefit (Models D and E vs. Model C). Also, using a 2D model only provided a small improvement (Model E vs. Model D), suggesting that a well-calibrated 1D model would be sufficient for long-term simulations at this field site, especially when considering the amount of effort required for more complex models.

Modelers should evaluate their particular situation to determine whether the increased effort of 2D heterogeneity and/or dual-porosity models is needed. However, due to the poor results of the most convenient model (Model A), it is highly discouraged to conduct any long-term simulations without first calibrating the model.

Acknowledgments

This research was funded by the Department of Biological Systems Engineering at the University of Nebraska–Lincoln, the Water for Food Global Institute at the University of Nebraska, and the USDA National Institute of Food and Agriculture, Hatch Project no. 1009760. The authors would also like to thank Dr. Garey Fox, North Carolina State University, for his input on this research. Dr. Chad Penn, USDA-ARS, provided a technical review of an earlier version of this manuscript. Ms. Ronica Stromberg provided a detailed editorial review of the manuscript.

References

- Akay, O., G.A. Fox, and J. Šimůnek. 2008. Numerical simulation of flow dynamics during macropore–subsurface drain interactions using HYDRUS. *Vadose Zone J.* 7:909–918. doi:10.2136/vzj2007.0148
- Alletto, L., Y. Coquet, P. Vachier, and C. Labat. 2006. Hydraulic conductivity, immobile water content, and exchange coefficient in three soil profiles. *Soil Sci. Soc. Am. J.* 70:1272–1280. doi:10.2136/sssaj2005.0291
- Beven, K., and P. Germann. 1982. Macropores and water flow in soils. *Water Resour. Res.* 18:1311–1325. doi:10.1029/WR018i005p01311
- Beven, K., and P. Germann. 2013. Macropores and water flow in soils revisited. *Water Resour. Res.* 49:3071–3092. doi:10.1002/wrcr.20156
- Cheviron, B., and Y. Coquet. 2008. Sensitivity analysis of HYDRUS-1D to transient-MIM parameters: A case study related to pesticide fate in soil. In: J. Šimůnek and R. Kodešová, editors, *Proceedings of the 2nd HYDRUS Workshop*. Prague, Czech Republic. 28 Mar. 2008. PC Progress, Prague. p. 27–34.
- Cooper, A.B., C.M. Smith, and M.J. Smith. 1995. Effects of riparian set-aside

- on soil characteristics in an agricultural landscape: Implications for nutrient transport and retention. *Agric. Ecosyst. Environ.* 55:61–67. doi:10.1016/0167-8809(95)00605-R
- Correll, D.L. 1999. Phosphorus: A rate limiting nutrient in surface waters. *Poult. Sci.* 78:674–682. doi:10.1093/ps/78.5.674
- DeLaune, P.B., P.A. Moore, Jr., D.K. Carman, A.N. Sharpley, B.E. Haggard, and T.C. Daniel. 2004. Development of a phosphorus index for pastures fertilized with poultry litter: Factors affecting phosphorus runoff. *J. Environ. Qual.* 33:2183–2191. doi:10.2134/jeq2004.2183
- Djordjic, F., K. Borling, and L. Bergstrom. 2004. Phosphorus leaching in relation to soil type and soil phosphorus content. *J. Environ. Qual.* 33:678–684. doi:10.2134/jeq2004.6780
- Elmi, A., J.S.A. Nohra, C.A. Madramootoo, and W. Hendershot. 2012. Estimating phosphorus leachability in reconstructed soil columns using HYDRUS-1D model. *Environ. Earth Sci.* 65:1751–1758. doi:10.1007/s12665-011-1154-1
- Fetter, C.W. 1999. *Contaminant hydrogeology*. 2nd ed. Waveland, Long Grove, IL.
- Fox, G.A., D.M. Heeren, R.B. Miller, A.R. Mittelstet, and D.E. Storm. 2011. Flow and transport experiments for a streambank seep originating from a preferential flow pathway. *J. Hydrol.* 403:360–366. doi:10.1016/j.jhydrol.2011.04.014
- Freiberger, R.P. 2014. Single- and dual-porosity calibration and long-term modeling of highly conductive floodplain soils in the Ozark ecoregion. M.S. thesis, Univ. of Nebraska, Lincoln, NE.
- Fuchs, J.W., G.A. Fox, D.E. Storm, C.J. Penn, and G.O. Brown. 2009. Subsurface transport of phosphorus in riparian floodplains: Influence of preferential flow paths. *J. Environ. Qual.* 38:473–484. doi:10.2134/jeq2008.0201
- Gburek, W.J., E. Barberis, P.M. Haygarth, B. Kronvang, and C. Stamm. 2005. Phosphorus mobility in the landscape. In: Sims, J.T. and A.N. Sharpley, editors, *Phosphorus: Agriculture and the environment*. *Agron. Monogr.* 46. ASA, CSSA, and SSSA, Madison, WI. p. 941–979. doi:10.2134/agronmonogr46.c29
- González-Delgado, A.M., and M.K. Shukla. 2014. Transport of nitrate and chloride in variably saturated porous media. *J. Irrig. Drain. Eng.* 140(5). doi:10.1061/(ASCE)IR.1943-4774.0000725
- Gotovac, H., V. Cvetkovic, and R. Andricevic. 2009. Flow and travel time statistics in highly heterogeneous porous media. *Water Resour. Res.* 45:W07402. doi:10.1029/2008WR007168
- Haws, N.W., P. Rao, C. Suresh, J. Šimůnek, and I.C. Poyer. 2005. Single-porosity and dual-porosity modeling of water flow and solute transport in subsurface-drained fields using effective field-scale parameters. *J. Hydrol.* 313:257–273. doi:10.1016/j.jhydrol.2005.03.035
- Heeren, D.M., G.A. Fox, C.J. Penn, T. Halihan, D.E. Storm, and B.E. Haggard. 2017. Impact of macropores and gravel outcrops on phosphorus leaching at the plot scale in silt loam soils. *Trans. ASABE* 60:823–835. doi:10.13031/trans.12015
- Heeren, D.M., G.A. Fox, and D.E. Storm. 2014. Berm method for quantification of infiltration at the plot scale in high conductivity soils. *J. Hydrol. Eng.* 19(2). doi:10.1061/(ASCE)HE.1943-5584.0000802
- Heeren, D.M., G.A. Fox, and D.E. Storm. 2015. Heterogeneity of infiltration rates in alluvial floodplains as measured with a berm infiltration technique. *Trans. ASABE* 58:733–745. doi:10.13031/trans.58.11056
- Lallemant-Barres, P., and P. Peaudecerf. 1978. Recherche des relations entre la valeur de la dispersivité macroscopique d'un milieu aquifere, ses autres caracteristiques et les conditions de mesure, etude bibliographique. *Bull. Bur. Rech. Geol. Min.* 3/4:277–287.
- Lamy, E., L. Lassabatere, B. Bechet, and H. Andrieu. 2009. Modeling the influence of an artificial macropore in sandy columns on flow and solute transfer. *J. Hydrol.* 376:392–402. doi:10.1016/j.jhydrol.2009.07.048
- Legates, D.R., and G.J. McCabe. 1999. Evaluating the use of “goodness-of-fit” measures in hydrologic and hydroclimatic model validation. *Water Resour. Res.* 35:233–241. doi:10.1029/1998WR900018
- Lopez, C.B., E.B. Jewett, Q. Dortch, B.T. Walton, and H.K. Hudnell. 2008. Scientific assessment of freshwater harmful algal blooms. Interagency Working Group on Harmful Algal Blooms, Hypoxia, and Human Health of the Joint Subcommittee on Ocean Science and Technology, Washington, DC.
- McPherson, R.A., C. Fiebrich, K.C. Crawford, R.L. Elliott, J.R. Kilby, D.L. Grimsley, et al. 2007. Statewide monitoring of the mesoscale environment: A technical update on the Oklahoma Mesonet. *J. Atmos. Ocean. Technol.* 24:301–321. doi:10.1175/JTECH1976.1
- Miller, R.B., D.M. Heeren, G.A. Fox, T. Halihan, and D.E. Storm. 2016. Heterogeneity influences on stream water-groundwater interactions in a gravel-dominated floodplain. *Hydrol. Sci. J.* 61:741–750. doi:10.1080/02626667.2014.992790
- Miller, R.B., D.M. Heeren, G.A. Fox, T. Halihan, D.E. Storm, and A.R. Mittelstet. 2014. The hydraulic conductivity structure of gravel-dominated vadose zones within alluvial floodplains. *J. Hydrol.* 513:229–240. doi:10.1016/j.jhydrol.2014.03.046
- Mittelstet, A.R., D.M. Heeren, D.E. Storm, G.A. Fox, M.J. White, and R.B. Miller. 2011. Comparison of subsurface and surface runoff phosphorus transport rates in alluvial floodplains. *Agric. Ecosyst. Environ.* 141:417–425. doi:10.1016/j.agee.2011.04.006
- Mittelstet, A.R., and D.E. Storm. 2016. Quantifying legacy phosphorus using a mass balance approach and uncertainty analysis. *J. Am. Water Resour. Assoc.* 52(12):1297–1310. doi:10.1111/1752-1688.12453
- Moriasi, D.N., J.G. Arnold, M.W. Van Liew, R.L. Bingner, R.D. Harmel, and T.L. Veith. 2007. Model evaluation guidelines for systematic quantification of accuracy in watershed simulations. *Trans. ASABE* 50:885–900. doi:10.13031/2013.23153
- Najm, M.R., J.D. Jabro, W.M. Iverson, R.H. Mohtar, and R.G. Evans. 2010. New method for the characterization of three-dimensional preferential flow paths in the field. *Water Resour. Res.* 46:W02503. doi:10.1029/2009WR008594
- Naseri, A.A., Y. Hoseini, H. Moazed, F. Abbasi, H.M.V. Samani, and S.A. Sakebi. 2011. Phosphorus transport through a saturated soil column: Comparison between physical modeling and HYDRUS-3D outputs. *J. Appl. Sci.* 11:815–823. doi:10.3923/jas.2011.815.823
- Nash, J.E., and J.V. Sutcliffe. 1970. River flow forecasting through conceptual models: 1. A discussion of principles. *J. Hydrol.* 10:282–290. doi:10.1016/0022-1694(70)90255-6
- Nimmo, J.R. 2010. Theory for source-responsive and free-surface film modeling of unsaturated flow. *Vadose Zone J.* 9:295–306. doi:10.2136/vzj2009.0085
- OCES. 2013. Using poultry litter as fertilizer. PSS-2246. Oklahoma State Univ., Stillwater. <http://poultrywaste.okstate.edu/Publications/files/pss-2246web.pdf> (accessed May 2014).
- Osborne, L.L., and D.A. Kovacic. 1993. Riparian vegetated buffer strips in water quality restoration and stream management. *Freshwater Biol.* 29:243–258. doi:10.1111/j.1365-2427.1993.tb00761.x
- Radcliffe, D.E., and J. Šimůnek. 2010. *Soil physics with HYDRUS: Modeling and applications*. CRC, Boca Raton, FL.
- Šimůnek, J., N.J. Jarvis, M.Th. van Genuchten, and A. Gärdenäs. 2003. Review and comparison of models for describing non-equilibrium and preferential flow and transport in the vadose zone. *J. Hydrol.* 272:14–35. doi:10.1016/S0022-1694(02)00252-4
- Šimůnek, J., and M.Th. van Genuchten. 2008. Modeling nonequilibrium flow and transport processes using HYDRUS. *Vadose Zone J.* 7:782–797. doi:10.2136/vzj2007.0074
- Šimůnek, J., M.Th. van Genuchten, and M. Šejna. 2012. The HYDRUS software package for simulating two- and three-dimensional movement of water, heat, and multiple solutes in variably-saturated media. *Tech. Manual, Version 2.0*. PC Progress, Prague.
- Šimůnek, J., M.Th. van Genuchten, and M. Šejna. 2016. Recent developments and applications of the HYDRUS computer software packages. *Vadose Zone J.* 15(7). doi:10.2136/vzj2016.04.0033
- Smith, D.R., K.W. King, L. Johnson, W. Francesconi, P. Richards, D. Baker, et al. 2015. Surface runoff and tile drainage transport of phosphorus in the Midwestern United States. *J. Environ. Qual.* 44:495–502. doi:10.2134/jeq2014.04.0176
- USEPA. 2015. Clean Water Act Section 303(d): Impaired waters and TMDL information. USEPA. <https://www.epa.gov/tmdl> (accessed December 2017).